A simplified edge illumination set-up for quantitative phase contrast mammography with synchrotron radiation at clinical doses

Mariaconcetta Longo[1], Luigi Rigon[2,3], Frances C. M. Lopez[2,3], Rongchan Chen[3,4], Diego Dreossi[5], Fabrizio Zanconati[6], Renata Longo[2,3]

[1]Post graduate school of Medical Physics, La Sapienza University of Rome, 00171 Rome, Italy
[2]Physics Department, University of Trieste, Via Valerio 2, 34127 Trieste, Italy
[3]Istituto Nazionale di Fisica Nulceare, Sezione di Trieste, Via Valerio 2, 34127 Trieste, Italy
[4]Shanghai Institute of Applied Physics, Chinese Academy of Sciences, Shanghai 201204, China
[5]Sincrotrone Trieste SCpA, S.S. 14 km 163.5, 34012 Basovizza Trieste, Italy
[6]Unità Clinica Operativa di Citodiagnostica e Istopatologia, Università degli Studi di Trieste, Trieste, Italy

E-mail: longo.mariaconcetta@gmail.com

Abstract. This work presents the first study of X-ray phase contrast imaging based on a simple implementation of the edge illumination method (EIXPCi) in the field of mammography with synchrotron radiation. A simplified EIXPCi set-up was utilized to study a possible application in mammography at clinical doses. Moreover, through a novel algorithm capable of separating and quantifying absorption and phase perturbations of images acquired in EIXPCi modality, it is possible to extract quantitative information on breast images allowing an accurate tissue identification. The study was carried out at the SYRMEP beamline of Elettra synchrotron radiation facility (Trieste, Italy), where a mastectomy specimen was investigated with the EIXPCi technique. The sample was exposed at three different energies suitable for mammography with synchrotron radiation in order to test the validity of the novel algorithm in extracting values of linear attenuation coefficients integrated over the sample thickness. It is demonstrated that the quantitative data are in good agreement with the theoretical values of linear attenuation coefficients calculated on the hypothesis of breast with a given composition. The results are promising and encourage the current efforts to apply the method in mammography with synchrotron radiation.

Submitted to: *Phys. Med. Biol.*

1. Introduction

In conventional X-ray imaging, contrast arises from differences in attenuation of X-rays between different tissues. In addition to absorption-based X-ray imaging, over the last two decades other techniques devoted to exploit the wave nature of X-ray were developed to enhance visibility of details and increase image contrast. These methods are called Phase Contrast imaging (PCi) techniques and were developed in order to obtain high contrast and high spatial resolution images of biological samples. This feature has proven useful in medical applications, with particular interest in mammography [1]. Differently from absorption-based methods, X-ray Phase Contrast imaging (XPCi) uses the phase shift induced by the sample as the source of image contrast. Moreover, as it is impossible to detect the phase shift directly, a method to convert the phase shift into a change of X-ray intensity is necessary [2] [3]. Many such methods have been developed and they can be classified in three main categories: interferometry with a crystal interferometer or with a Talbot (grating) interferometer, Analyzer Based Imaging (ABI) which is based on the use of an analyzer crystal, and free-space propagation [4]. The main difference between the above methods is in the detected physical quantity: the crystal interferometer measures the phase shift (Φ) directly, the analyzer-based imaging method and the Talbot interferometry detect the first spatial derivative of the phase (or phase gradient) ($\nabla\Phi$), while in propagation-based phase imaging the measured quantity corresponds to the second derivative (Laplacian of the phase) ($\Delta\Phi$) [3]. Even though these methods are fascinating, they suffer from some limitations regarding their application into the clinical practice. On the one hand, these constraints can include need of coherent sources and mechanical stability; on the other hand, some techniques deliver dose inefficiently, requiring long acquisition times, with fields of view currently limited to few centimeters [4] [5].

To remove most limitations of the XPCi methods discussed above, Olivo and Speller proposed an alternative phase contrast technique called Coded Apertures X-ray Phase Contrast imaging (CAXPCi), that uses two sets of appropriately positioned coded aperture masks to enhance image contrast [6]. In CAXPCi, instead of generating an interference pattern such as free space propagation or grating-based interferometer, which leads to substantial source coherence requirements, the effect of X-ray refraction is maximised. The basic idea comes from a SR experiment carried out by Olivo et al. [7], who observed that the phase sensitivity of an imaging system can be strongly enhanced by illuminating only the edge of the active surface of the detector pixel, with a small fraction of the beam cross section falling outside the pixel edge itself. This principle is known as edge illumination XPCi (EIXPCi) and imaging can be done by scanning the sample through the beam. Using the CAXPCi techniques the sample scanning used in SR imaging becomes unnecessary and it is replaced by the use of an area detector. In order to do this, the arrangement used for EIXPCi has to be repeated for every detector row (or column), using two sets of specifically designed coded aperture system [8].

An image processing technique closely related to XPCi is phase retrieval [9]. If XPCi

is an imaging modality developed with the aim of enhancing the total contrast of the images through the phase shift introduced by the object (human body part), phase retrieval is a mathematical technique to extract the quantitative phase shift map from XPC images [10] [11]. Different phase-retrieval algorithms have been developed in the field of X-ray imaging. In the field of EIXPCi, Munro et al. [12] developed an algorithm for separating and quantifying the absorption and the gradient of the phase shift due to a sample imaged using the EIXPCi system. We refer to the theoretical model presented in detail in a recent publication [13] and employed later to separate information about absorption and phase contrast effects. This method, based on a double acquisition in EIXPC modality, works on the inversion of the equations which calculate the signals I_+, that results in a detected signal which is obtained covering the detector pixel with a mask so that it is illumined by the 50% of the beam from the bottom side, and I_-, that results in a detected signal obtained illumining the pixel with the 50% of the beam from the top side [12]. The algorithm was verified by acquiring images of different absorbing wires using a synchrotron radiation source and a single photon counting detector providing an high dynamic range, low noise and an almost ideal Line Spread Function (LSF); it works well in the proximity of large phase and absorption gradients. The application of this latter method could lead to higher image quality and to the possibility of more accurate material identification. Differently from conventional radiography, which allows to extract only information related to absorption, the application of phase retrieval algorithm leads to images that are quantitative maps of absorption and differential phase. Even if this mathematical algorithm was tested on simple samples as wires [14] [15] [16], it can be transferred in principle to mammography.
Here, the main aim is to use maps of absorption and differential phase to extract quantitative information on the composition of breast in order to differentiate tissues. Moreover, this method can be applied while delivering doses compatible with clinical mammography. Therefore, in order to test a clinically viable set-up for mammography, a compromise between the set-up complexity (including alignment requirements) and image contrast was sought.

2. Materials and methods

2.1. Phase retrieval algorithm

The phase retrieval algorithm by Munro et al. [12] is based on the acquisition of signals in two complementary EIXPCi configurations, I_+ and I_- (Figure 1).
Arranging the two acquired signals, the algorithm is capable to extract:

$$\mu(\xi_s) = log\left[\frac{I_0}{(I_+ + I_-)|^{\xi_i=0}}\right] \tag{1}$$

$$\frac{1}{k}\frac{\partial\Phi}{\partial\xi}\Big|^{\xi_s} = -\left[\frac{I_+ - I_-}{I_+ + I_-}\Big|^{\xi_i=0} + \frac{1}{4}\frac{\partial\mu}{\partial\xi}\Big|^{\xi_s} a_1\right]\frac{a_1(d_1+d_2)}{2d_1d_2} \tag{2}$$

where Φ and μ, both real valued, are defined as

$$\Phi(y) = k \int_O \delta(y,z)\, dz \qquad , \qquad \mu(y) = 2k \int_O \beta(y,z)\, dz \tag{3}$$

with δ and β the real and imaginary part of the refractive index n ($n = 1 - \delta + i\beta$) respectively, $k = 2\pi/\lambda$ the wave number for wavelength λ and O the extent of the object. The other symbols are defined in Figure 1: a_1 is the sample aperture, d_1 the source to sample distance, d_2 the sample to detector distance, while ξ_s is used to represent the shift of the sample with respect to the detector pixel along y direction.
Equation 1 represents the retrieved absorption (RA) image, which is a map of absorption integrated over the object, but also contains the so called extinction contrast, which originates from the rejection of small-angle scattering [17].
Equation 2 yields the differential phase (DP) image, which is a map of $(1/k)(\partial\Phi/\partial\xi)$ and therefore highlights the phase variations along the vertical (or scanning) direction.

Figure 1: The two complementary EIXPCi configurations used to perform quantitative EIXPCi. Note that ($\overline{x}$, $\overline{y}$, z), (ξ, ψ, z) and (x, y, z) represent the coordinate systems for source, sample and detector planes respectively and form a right handed coordinate systems. M is the system magnification factor given by $(d_1 + d_2)/d_1$. The diagrams are not to scale.

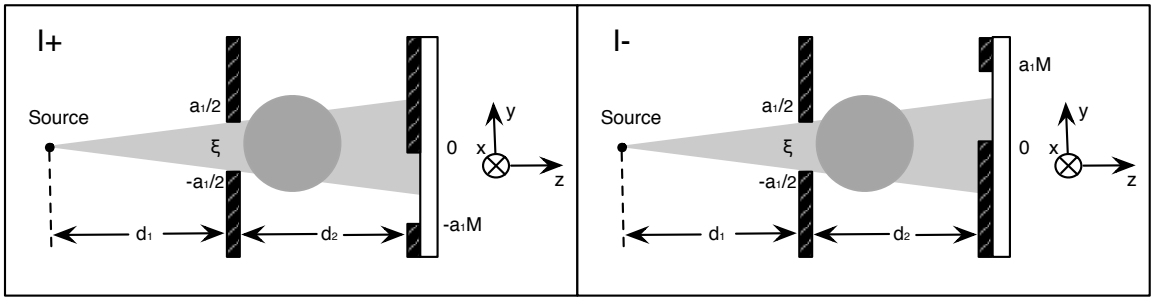

2.2. Simulations

Before defining a EIXPCi set-up suitable for medical application in the field of mammography, some simulations were performed in order to test the contrast behaviour as a function of the source dimension and of the fraction of pixel exposed to radiation, that will be indicated in the following as Illuminated Pixel Fraction (IPF). The simulations are based on the ray-optics approach, in which the deviation angle of the photon is obtained from the gradient of the real part of the refractive index inside the imaged object [6]. Two sets of simulations have to be discussed. In all cases, the source to sample distance and the sample to detector distance were fixed to 23 m and 1.5 m respectively, and the pixel size was set to 300 μm in order to reproduce the experimental

conditions described in the next session (2.3 *Experiment*).
Moreover, 5M photons histories have been used in all simulations, in order to achieve a negligible statistical error.
The first set of simulations was performed by keeping the IPF set to 50%, while the vertical dimension of the beam shaped by the sample slits was changed. The simulations were performed without slits in front of the detector and using the sharpness of the detector active surface itself (edge-on configuration, i.e. with only the edge of the detector illumined by the incoming beam) to enhance the phase sensitivity of the imaging system (see Figure 2) [18] [19]. A 200 μm diameter PEEK monofilament was used as sample and it was illuminated by 20 keV monochromatic radiation.
The second set of simulations was performed by keeping the vertical dimension of the beam shaped by the sample slits set to 100 μm, while various IPF were realized by shifting the detector.

2.3. Experiment

To provide a low dose absorption and differential phase mammography by means of the Munro's phase extraction technique, an experimental validation was performed at the SYRMEP bending magnet beamline of Elettra synchrotron radiation facility (Trieste, Italy). As a clinically viable set-up for mammography was tested, the beam size was not to be too small in order to have a sufficient number of photons for enabling short acquisition times. For these reasons, we considered a situation in which the beam is 100 μm high and half of it illuminates the detector in the edge-on configuration when the sample is not present. As the pixel size is 300 μm, this means that a fraction of about 17% of the detector is directly illuminated by the radiation. The imaging method required to set-up both I_+ and I_- configurations in order to apply the algorithm for extracting absorption and differential phase information. Munro's phase retrieval method uses two sets of masks, one shaping the beam, while the other covers the pixel in order to create and insensitive area of the detector pixel itself. For applying this method to mammographic examination, we propose a simplified set-up, which utilizes only one mask for shaping the beam, while the insensitive area of the detector pixel is created by using the edge of the pixel itself. Figure 2 represents a schematic view of the simplified experimental set-up arranged for testing the EIXPCi in mammography with synchrotron radiation. The source to sample distance was approximately 23 m and the sample to detector distance was set to 1.5 m, while the slits to sample distance was about 60 cm. The sample slits that shapes a 100 μm beam were used to form the pre-sample aperture, while the detector was positioned in the edge-on configuration. The vertical position of the detector was alternated between the I_+ and I_- positions.

Figure 2: Side-on view of the simplified experimental EIXPCi setup. The scheme is not scaled.

(a) I_+ configuration.

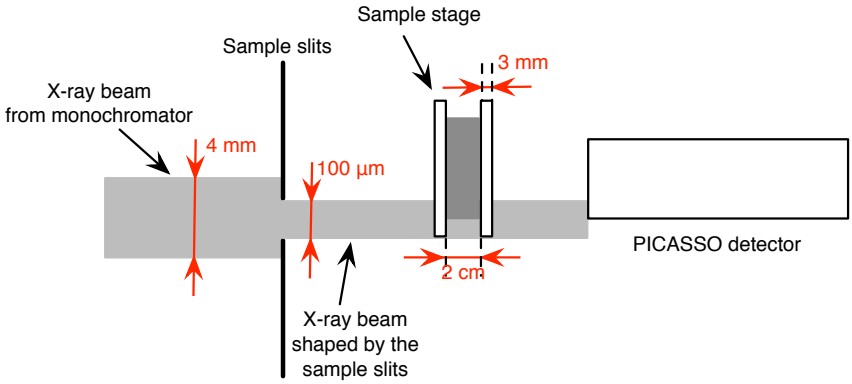

(b) I_- configuration.

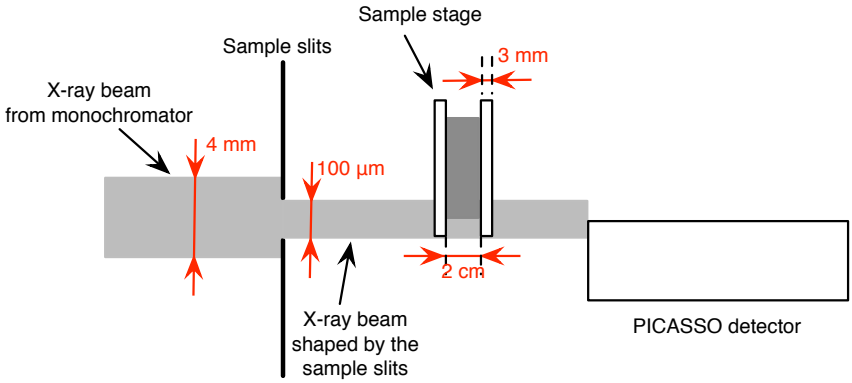

A microstrip silicon detector, operating in direct conversion and single photon counting mode, named PICASSO (Phase Imaging for Clinical Applications with Silicon detector and Synchrotron radiatiOn), was used [19] [20] [21]. This allowed also to maximize the contrast resolution and to overcome the limitation in the signal dynamic range, which are typical of charge-integration detectors. The PICASSO detector operates in the edge-on configuration, i.e. with the photons reaching the sensor on the thin side, parallel to the strips, that provides a high absorption efficiency thus reducing the dose delivered to the patient. The detector pixel size is defined by the 50 μm strip pitch horizontally and by the 300 μm sensor thickness vertically. The prototype meets the requirements for clinical mammography with synchrotron radiation as far as spatial resolution, contrast resolution, efficiency and acquisition speed are concerned, showing outstanding results on phantom studies [19] [20] [21].

The work described in this note has been carried out following the Directive 2004/23/EC of the European Parliament and of the Council of 31 March 2004 on setting standards of quality and safety for the donation, procurement, testing, processing, preservation,

storage and distribution of human tissues.
The images presented in this study were acquired in order to guide the pathologist in the localization of the lesions for the histological preparation, according to the standard procedures of the Cytodiagnosis and Histopathology Clinical Operational Unit of the University Hospital of Trieste, accredited by JCI (Joint Commission International). The sample was prepared from specimens of total mastectomy and was derived from surgical material sent to the Pathology Unit of the University Hospital of Trieste (Italy) according to local guidelines for histological examination. The removed breast specimens were marked with metal clips to unequivocally identify its 3-dimensional orientation. The sample was fixed in formalin and stored at room temperature. It contained an invasive carcinoma characterized by axillary lymph node metastases and with a tumor grading of G2-3. The specimen, consisting of a single 2 cm thick slices, were placed into vacuum bags and mounted inside two plexiglass supports, each 3 mm thick, for preventing sample movements (Figure 2). The dose was calculated on the basis of the flux registered on an ionization chamber. Imaging was performed by scanning the sample through the beam with a scan step of 50 μm; each acquisition took approximately 20 ms. When images were acquired at different energies, the scan speed was modified to keep the dose delivered to the specimens at constant level, with an entrance air kerma of about 1 mGy for one exposure. As two acquisition, I_+ and I_-, had to be performed, the latter dose corresponds to a half of the Entrance Skin Exposure (about 2 mGy) delivered during a SR mammography on a sample of comparable thickness [22].
The sample was imaged at energies of 17 keV, 20 keV and 23 keV.
Moreover, as the aim of this study is to characterize the materials using their absorption attenuation coefficient, an absorption image was acquired at 20 keV with the sample placed in close contact with the single photon counting PICASSO detector.

3. Results

3.1. Simulations results

In the following, the results of the simulations performed to test the image contrast by varying the beam size and the IPF are described. Firstly, the values of contrast as a function of the vertical dimension of the beam shaped by the sample slits were obtained and this is reported in the graph of Figure 3 (a). The contrast values were obtained as $(I_{max} - I_{min})/(I_{max} + I_{min})$, where I_{max} and I_{min} represent the maximum and the minimum intensities in the image profile of the simulated monofilament. As it can be seen, the contrast values decrease by increasing the vertical dimension of the beam used to illuminate the detector. Secondly, the possibility of shifting the detector in different positions, consequently illuminating different fractions of the pixel active surface, was explored. This is of extreme interest as there is previous evidence that a reduction of the illuminated fraction results in an increase in image contrast [5]. In Figure 3 (b), the contrast values for a 200 μm diameter PEEK monofilament illuminated by

20 keV monochromatic radiation are reported as function of different pixel-illuminated fractions. As the figure shows, the contrast values decrease when the fraction of pixel exposed to radiation is increased. The pixel size was set to 300 μm in all the simulation discussed above.

Figure 3: Influence of the beam size and of the IPF on the contrast.

(a) Contrast versus beam size.

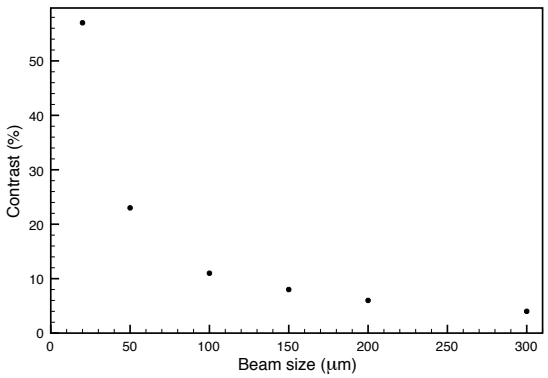

(b) Contrast versus illuminated pixel fraction.

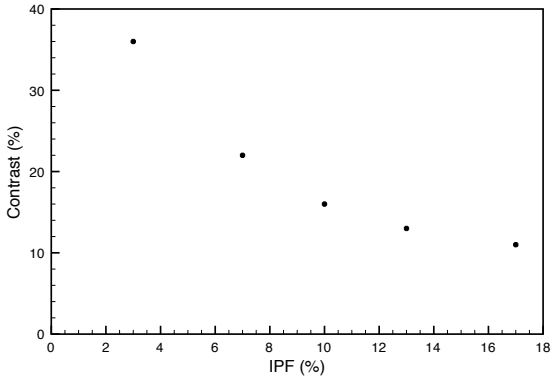

The simulations results depicted in Figure 3 do not show any local maxima, i.e. they do not indicate any preferred beam size or IPF value. Therefore, ideally one should use a beam size and an IPF as small as possible. However, in order to obtain a clinically viable set-up, characterized by short exposure times and relaxed alignment requirements, too small values had to be avoided. Thus, as previously described, a beam size of 100 μm and an IPF of 17% were chosen for the experiment. The results obtained in the simulation anyway assure that reasonably high contrast values are still achievable with such parameters.

3.2. Experimental data and phase retrieval results

Images acquired in the I_+ and I_- configurations as well as the RA and the DP images will be presented in the following. Moreover, a quantitative study on selected Regions Of Interest (ROIs) of retrieved absorption images of the specimen will be performed at different energies (17 keV, 20 keV and 23 keV). Figures 4 and 5 show the images (2.5×12 cm^2) of the studied specimen at 17 keV and 23 keV respectively. Some artefacts, i.e. horizontal stripes in the images, slightly affect image quality and can be caused by beam instabilities during the acquisition.

Figure 4: Images of the specimen acquired at 17 keV in EIXPCi configuration (a) (b). Retrieved absorption (c) and differential phase (d) images are obtained by applying the mentioned PR algorithm.

(a) I_+. (b) I_-. (c) RA. (d) DP.

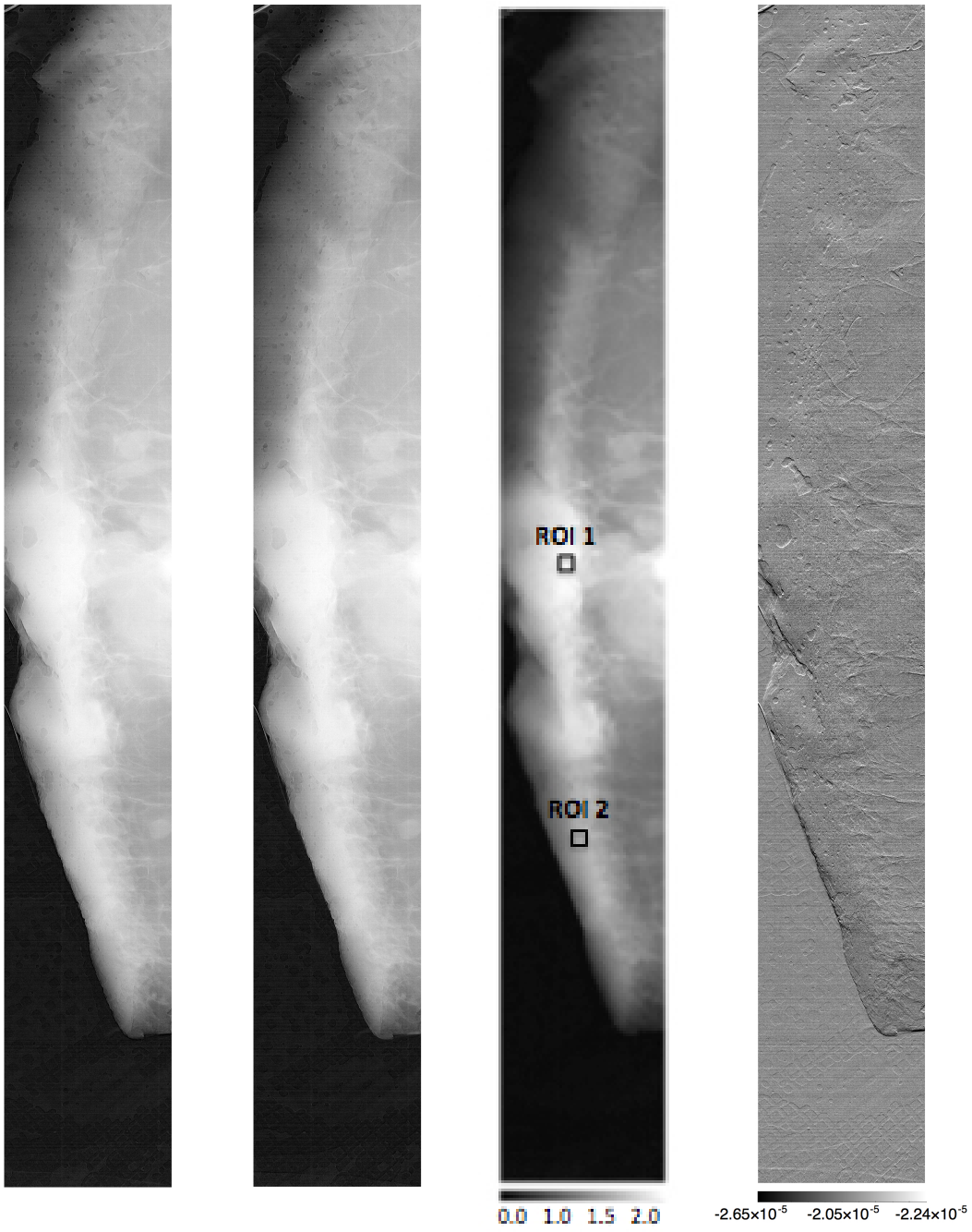

Figure 5: Images of the specimen acquired at 23 *keV* in EIXPCi configuration (a) (b). Retrieved absorption (c) and differential phase (d) images are obtained by applying the mentioned PR algorithm.

(a) I_+. (b) I_-. (c) RA. (d) DP.

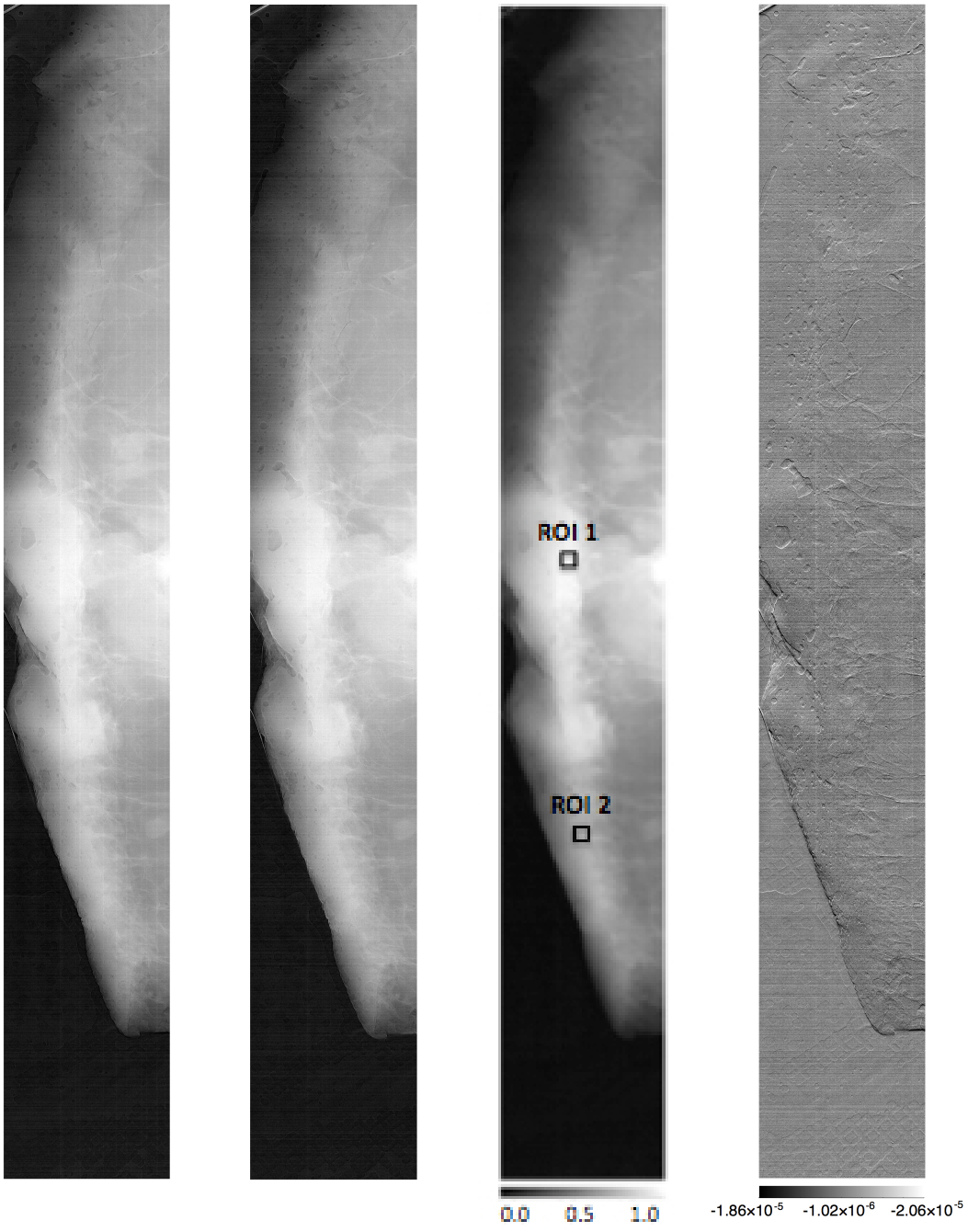

Table 1: Comparison between expected and measured values of $\mu \cdot x$. The expected values were calculated considering a tissue made of 50% of fibrous and 50% of fat tissue, a 100% fibrous tissue or a 100% fat tissue.

	$\mu \cdot x$ Expected			$\mu \cdot x$ Measured	
E (keV)	100% fibrous	50% fibrous 50% fat	100% fat	First ROI	Second ROI
17	2.97 ± 0.33	2.37 ± 0.26	1.77 ± 0.19	2.20 ± 0.04	1.60 ± 0.12
20	2.07 ± 0.23	1.69 ± 0.19	1.31 ± 0.14	1.51 ± 0.03	1.13 ± 0.08
23	1.54 ± 0.17	1.28 ± 0.14	1.03 ± 0.11	1.11 ± 0.03	0.87 ± 0.07

The retrieved absorption images represent a map of $\mu \cdot x$, where μ is the linear attenuation coefficient and x is the thickness of the sample. The mean values of different regions in the retrieved absorption images were compared with the expected ones, calculated taking into account the attenuation of the tissue and of the two plexiglass supports. For this purpose, two ROIs in two homogeneous regions inside the tissue were selected (Figure 4 (c) and 5 (c)) and their mean value and standard deviation were taken for the two studied energies. In order to calculate the expected value of $\mu \cdot x$, as we do not exactly know the tissue composition in the selected ROI, three different hypothesis were considered. The first one is that the tissue is made of 50% of fibrous and 50% of fat tissue, while the second and the third consider 100% fibrous and 100% fat tissue respectively. We referred to values of linear attenuation coefficient for fibrous and fat recently published [23], while the values of linear attenuation coefficient of plexiglass for different energies were extracted through the computer program XMuDat [24]. Table 1 shows the comparison between expected and measured values of $\mu \cdot x$ in the cases mentioned above. Errors on the expected values were calculated considering an uncertainty of 10% on the measured thickness of the sample and its supports. The comparison reveals that the values of $\mu \cdot x$ obtained for the first ROI are consistent with the hypothesis of a tissue made of 50% of fibrous and 50% of fat tissue, while the values of $\mu \cdot x$ obtained for the second ROI are similar to those expected for a 100% fat tissue. Moreover, no ROI, whose values correspond to the hypothesis that the breast tissue consist of 100% fibrous tissue, was found. Considering the uncertainties reported in Table 1, we can conclude that this method allowed to reasonably predict the composition of the breast tissue, as the map of $\mu \cdot x$ is retrieved.

A quantitative analysis was carried out on the same ROIs selected on the absorption image acquired by placing the sample in direct contact with the detector. This analysis produced on the first ROI a value of $\mu \cdot x = 1.39 \pm 0.20$, while on the second ROI $\mu \cdot x = 1.04 \pm 0.20$ which, even though systematically lower, are in agreement with both theoretical and RA values evaluated at 20 keV on the hypothesis of a tissue made of 50% of fibrous and 50% of fat tissue and of a 100% fat tissue respectively.

Figure 6 shows the absorption image acquired using a conventional digital mammography system compared to the retrieved absorption at 20 keV obtained by applying the phase retrieval approach. The conventional mammographic image was acquired with a Senographe DS (GE Healthcare, Chalfont St Giles, England) system operated at 26 kVp and 25 mAs; the entrance air kerma was 2 mGy.

Figure 6: Breast specimen image acquired using a conventional digital mammography system and the retrieved absorption obtained applying the phase retrieval approach to EIXPCi images acquired at 20 keV.

(a) Conventional. (b) RA.

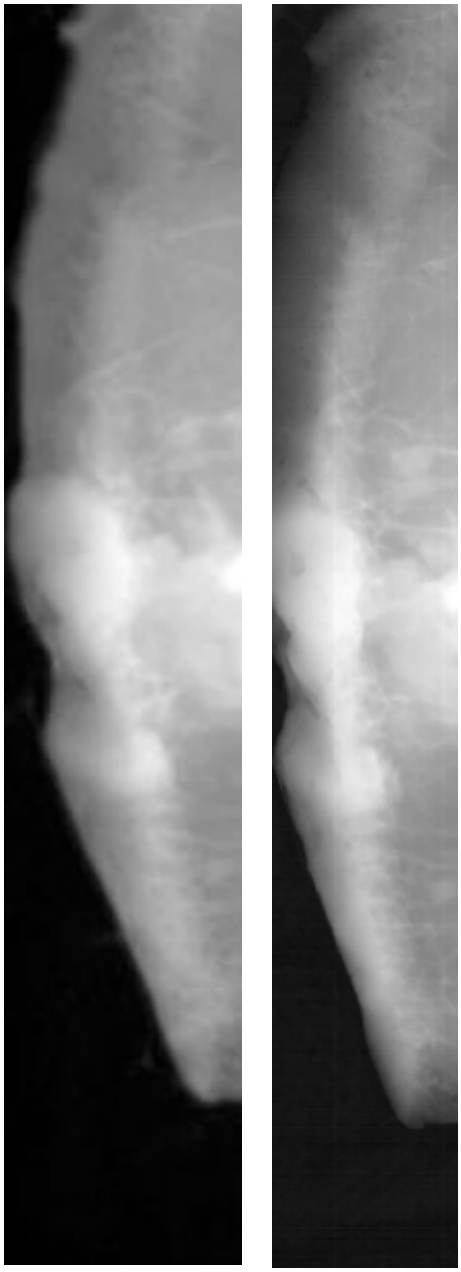

The latter images do not have the same horizontal dimensions as (a) was extracted from the image acquired using a conventional digital mammography system and (b) was retrieved for images acquired in EIXPCi modality, so that in the latter case the image dimension is affected by the source to sample distance causing a non negligible magnification. The images presented above look similar to each other, without artifacts introduced by the algorithm in RA image, demonstrating that the latter can provide also valuable qualitative information in addition to the quantitative one.

4. Discussion

For the first time, mastectomy specimens were investigated with a simplified EIXPCi technique and a SR source. Measurements were carried out under dose conditions close to those applied to the patients examined at the SYRMEP beamline [25] [26]. We were able to retrieve both absorption and differential phase maps from images acquired in the I_+ and I_- configurations at different energies.

As expected, the I_+ and I_- images show phase contrast effects superimposed to the conventional contrast due to the attenuation of X-rays. Such phase contrast effects can be noticed as an edge-enhancement of the tiny structures included in the breast specimen, and in particular of those structures which are mainly oriented along the horizontal direction, where the sensitivity of the EIXPCi technique is maximized. The phase retrieval allows to disentangle the attenuation and phase contrast effects, respectively in the RA and the DP image. The RA image is rather similar to a conventional image (although it contains an additional pool of contrast, due to extinction, i.e. the rejection of small angle scattering [17]), and therefore can be immediately appreciated by a radiologist. On the contrary, the DP image has little resemblance to conventional mammography, and its diagnostic interpretation is therefore less obvious. However, it should be pointed out that the DP image can depict tiny structures (particularly those characterized by horizontal edges) and can thus provide complementary information to the RA image. Of note, the DP image seems to be more sensitive than the RA image to artifacts due to the instability of the beam, as can be appreciated in Figure 4 (d) and 5 (d).

There are different factors which affect the phase retrieval mechanism in the experimental configuration previously discussed. One can be ascribed to the main difference between the set-up using both sample and detector masks and the simplified one we used. In a typical CAXPCi set-up that uses both sample and detector apertures, when the detector is in the I_+ configuration, the bottom half of the detector pixel registers counts and it can be considered as active portion. Otherwise, when the detector is in the I_- configuration, the active portion of the detector pixel is the half on the top. In this way, two complementary situations are reached, and all the detector pixel is exploited in two acquisitions. When the simplified set-up is used, the counts are registered by the entire pixel both in the I_+ and I_- configurations. The two configurations are still complementary, but the initial condition of the phase retrieval

approach is not exactly satisfied. In other words, the main difference between the two methods is that in the simplified one the entire pixel is exploited twice, i.e. once in the I_+ and once in the I_- configurations. Moreover, as the insensitive area of the detector pixel is created by using the edge of the pixel itself, in order to acquire images in two complementary conditions, the detector LSF should be as symmetric as possible. This doesn't happen in our experiment as the PICASSO vertical LSF is not perfectly symmetric, as Figure 7 shows. The LSF FWHM corresponds to the vertical dimension of the detector pixel that is 300 μm. This asymmetry is due to the presence of an asymmetric dead zone in the PICASSO detector [19], which affects the shape of the detector LSF. As a matter of fact, in order to limit the dark current, the strip implants are kept at about 0.2 mm distance from the detector physical edge, which represents the beam entrance window in the edge-on geometry. Thus a dead zone is determined, where the impinging photons may interact without being detected, slightly decreasing the detector intrinsic efficiency (which is of the order of 80% in the X-ray energy range from 19 to 21 keV [19]). Moreover, since the dead zone is deeper at the strip side than at the backplane, the symmetry of the detector LSF is also somewhat affected.

Figure 7: Detector LSF. Each step is 10 μm.

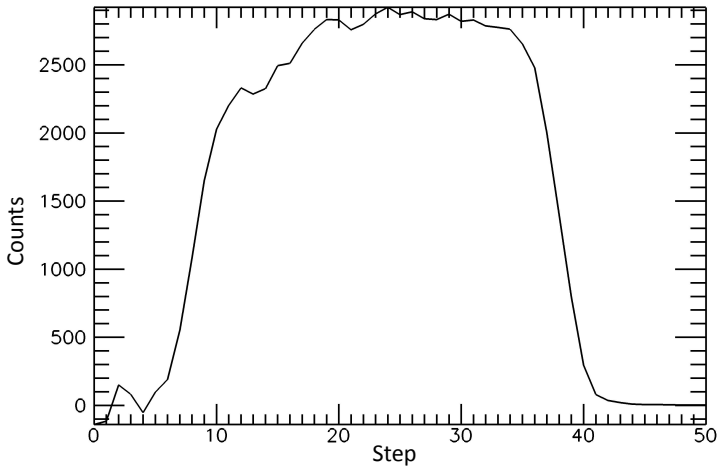

Even though the retrieved absorption and differential phase images could be affected by these limitations, this study shows that the Munro's algorithm works well in extracting quantitative information on retrieved absorption images. Our results are demonstrated to be in good agreement with the theoretical values of linear attenuation coefficients calculated for a breast with a given composition. Moreover, the values of $\mu \cdot x$ obtained on the absorption image acquired at 20 keV by using the PICASSO detector agree with the corresponding values calculated on the RA image and theoretically expected, even though they are systematically lower; this trend can be attributed to the presence of scattered radiation and to absence of the extinction contrast in the

absorption image.
Other improvements can be achieved with regards to the dose delivered to the specimens. To optimize the dose, the width of the beam not hitting the detector could be reduced, i.e. smaller than the one which impinges on the detector pixel. In this way, a balance between an optimised dose and the SNR (Signal to Noise Ratio) could be achieved.

5. Conclusion

The novelty of quantitative phase contrast mammography lies in the possibility to obtain quantitative information on the nature of the breast tissue from retrieved absorption images, that is not possible with current mammographic examinations. Given the evident advantage of extracting such information, associated to maps of retrieved absorption and/or differential phase, it is expected that the EIXPCi phase retrieval method could be useful in mammography to reasonably predict the composition of breast tissue. In the present study a simplified set-up for EIXPCi was used in order to study a mastectomy sample and the Munro's algorithm was applied. Our results demonstrate that Munro's algorithm is robust and it can be useful to obtain quantitative breast maps even when working at acceptable doses and in non-ideal conditions. Higher quality maps can be obtained using the original EIXPCi set-up, i.e. using a couple of slits, the first close to the patient and the second in front of the detector in order to obtain a sharp beam and a symmetric pixel sensitivity profile.
In vivo applications require large field of view and limited time for fine alignment during exams or between one patient and the following: therefore a compromise will be necessary. Our experience indicates that EIXPCi is a good candidate for clinical quantitative phase contrast imaging, giving reliable quantitative maps even with poor geometry and low dose.

Acknowledgments

The authors thank Prof. Olivo, University College London, UK, and Dr. Munro, University of Western Australia, Australia, for the useful discussions.
F. C. M. Lopez acknowledges the financial grant from the Brautti family and the ICTP TRIL program.

References

[1] F. Arfelli, M. Assante, V. Bonvicini, A. Bravin, G. Cantatore, E. Castelli, L. Dalla Palma, M. Di Michiel, R. Longo, A. Olivo, S. Pani, D. Pontoni, P. Poropat, M. Prest, A. Rashevsky, G. Tromba, A. Vacchi, E. Vallazza and F. Zanconati (1998), *Low-dose phase contrast X-ray medical imaging*, Phys. Med. Biol., Vol. 43, 2845–2852.

[2] Y. Akio, W. Jin, H. Kazuyuki, T. Tohoru (2008), *Quantitative comparison of imaging performance of x-ray interferometric imaging and diffraction enhanced imaging*, Med. Phys., Vol. 35, 4724.

[3] R. Fitzgerald (2000), *Phase Sensitive X-Ray Imaging*, Phys. Today, Vol. 53, 23-27.

[4] A. Bravin, P. Coan, P. Suortti (2013), *X-ray phase contrast imaging from pre-clinical applications towards clinics*, Phys. Med. Biol., Vol. 58, R1-R35.

[5] A. Olivo, S. Gkoumas, M. Endrizzi, C. K. Hagen, M. B. Szafraniec, P. C. Diemoz (2013), *Low-dose phase contrast mammography with conventional x-ray sources*, Med. Phys., Vol. 40, No. 9.

[6] A. Olivo and R. Speller (2007), *Modelling of a novel x-ray phase contrast imaging technique based on coded apertures*, Phys. Med. Biol., Vol. 52, 6555-6573.

[7] A. Olivo, F. Arfelli, G. Cantatore, R. Longo, R. Menk, S. Pani, M. Prest, P. Poropat, L. Rigon, G: Tromba, E. Vallazza and E. Castelli (2001), *An innovative digital imaging set-up allowing a low-dose approach to phase contrast applications in the medical field*, Med. Phys., Vol. 28, 1609-1610.

[8] A. Olivo and R. Speller (2008), *Image formation principles in coded-aperures based x-ray phase contrast imaging*, Phys. Med. Biol., Vol. 53, 6461-6474.

[9] X. Wu and H. Liu (2007), *Clarification of aspects in in-line phase sensitive x-ray imaging*, Med. Phys., Vol. 34, 737–743.

[10] K. A. Nugent (2007), *X-ray noninterferometric phase imaging: an unified picture*, J. Opt. Soc. Am. A 24, 536-547.

[11] L. De Caro, F. Scattarella, C. Giannini, S. Tangaro, L. Rigon, R. Longo and R. Bellotti (2010), *Combined mixed approach algorithm for in-line phase-contrast x-ray imaging*, Med Phys., Vol. 37, 3817-3827.

[12] P. Munro, L. Rigon, K. Ignatyev, F. C. Lopez, D. Dreossi, R. Speller and A. Olivo (2013), *A quantitative, non-interferometric X-ray phase contrast imaging technique*, Opt. Exp., Vol. 21, No. 1, 647-661.

[13] P. Munro, K. Ignatyev, A. Olivo and R. Speller (2010), *The relationship between wave and geometrical optics models of coded aperture type x-ray phase contrast imaging systems*, Opt. Exp., Vol. 18, 4103.

[14] P. R. T. Munro, C. K. Hagen, M. B. Szafraniec, A. Olivo (2013), *A simplified approach to quantitative coded aperture X-ray phase imaging*, Opt. Exp., Vol. 21, 11187-20.

[15] C. K. Hagen , P. C. Diemoz, M. Endrizzi, L. Rigon, D. Dreossi, F. Arfelli, F. C. M. Lopez, R. Longo, A. Olivo (2014), *Theory and preliminary experimental verification of quantitative edge illumination x-ray phase contrast tomography*, Opt. Exp., Vol. 22, 7989-8000.

[16] C. K. Hagen, P. R. T. Munro, M. Endrizzi, P. C. Diemoz, A. Olivo (2014), *Low-dose phase contrast tomography with conventional x-ray sources*, Med. Phys., Vol. 41, 070701.

[17] D. Chapman, W. Thomlinson, R. E. Johnston, D. Washburn, E. Pisano, N. Gmur, Z. Zhong, R. Menk, F. Arfelli, D. Sayers (1997), *Diffraction enhanced x-ray imaging*, Phys. Med. Biol., Vol. 42, 2015.

[18] F.C. Lopez, L. Rigon, R. Longo, F. Arfelli, A. Bergamaschi, R.C. Chen, D. Dreossi, B. Schmitt, E. Vallazza and E. Castelli (2011), *Development of a fast read-out system of a single photon counting detector for mammography with synchrotron radiation*, J. Inst. 6, C12031.

[19] L. Rigon, F. Arfelli, F. Astolfo, A. Bergamaschi, D. Dreossi, R Longo, R.H. Menk, B. Schmitt, E. Vallazza and E. Castelli (2009), *A single photon counting edge-on silicon detector for synchrotron radiation mammogrphy*, Nucl. Instr. and Meth., Vol. A 628, S62-5.

[20] A. Mozzanica, A. Bergamaschi, R. Dinapoli, F. Gozzo, B. Henrich, P. Kraft, B. Patterson, B. Schmitt (2009), *MythenII: A 128 single photon counting readout chip*, Nucl. Instrum. Meth. A 607, 250.

[21] F.C. Lopez, L.Rigon, L. Fadin, F. Arfelli, A. Bergamaschi, D. Dreossi, M. Longo, B. Schmitt, E. Vallazza, E. Castelli, R. Longo (2014), *Comparator threshold settings and the effective pixel size of the PICASSO detector, Journal of Instrumentation*, J. Inst. 9, C05056.

[22] E. Quai, R. Longo, F. Zanconati, G. Jaconelli, M. Tonutti, A. Abrami, F. Arfelli, D. Dreossi, G. Tromba, M. A. Cova (2011), *First application of computed radiology to mammography with synchrotron radiation*, Rad. med. DOI 10.1007/s11547-012-0847-1.

[23] R. C. Chen, R. Longo, L. Rigon, F. Zanconati, A. De Pellegrin, F. Arfelli, D. Dreossi, R. Menk, E.

Vallazza, T. Q. Xiao and E. Castelli (2010), *Measurement of the linear attenuation coefficients of breast tissues by synchrotron radiation computed tomography*, Phys. Med. Biol., Vol. 55, 4993-5005.

[24] Nowotny R. XMuDat: Photon attenuation data on PC. IAEA-NDS-195 International Atomic Energy Agency, Vienna, Austria. 1998. Available from: http://www.mds.iaea.or.at/reports/mds-195.htm.

[25] E. Castelli, M. Tonutti, F. Arfelli, R. Longo, E. Quaia, L. Rigon, D. Sanabor, F. Zanconati, D. Dreossi, A. Abrami, E. Quai, P. Bregant, K. Casarin, V. Chenda, R. H. Menk, T. Rokvic, A. Vascotto, G. Tromba, M. A. Cova (2010), *Mammography with synchrotron radiation: first clinical experience with phase-detection technique*, Radiology 259(3):684-94.

[26] R. Longo, M. Tonutti, L. Rigon, F. Arfelli, D. Dreossi, E. Quai, F. Zanconati, E. Castelli, G. Tromba, M. A. Cova (2014), *Clinical study in phase- contrast mammography: image-quality analysis*, Phil. Trans. R. Soc. A 372.